High and low thermal conductivity of amorphous macromolecules

Xu Xie, Kexin Yang, Dongyao Li, Tsung-Han Tsai, Jungwoo Shin, Paul V. Braun, and David G. Cahill

Phys. Rev. B **95**, 035406 — Published 9 January 2017

DOI: 10.1103/PhysRevB.95.035406

High and low thermal conductivity of amorphous macromolecules

Xu Xie,[1†*] Kexin Yang,[2†] Dongyao Li,[1] Tsung-Han Tsai,[1] Jungwoo Shin,[1] Paul V. Braun,[1] David G. Cahill[1]

[1]*Department of Materials Science and Engineering, Frederick Seitz Materials Research Laboratory, University of Illinois at Urbana-Champaign, Urbana, Illinois 61801, USA.*

[2]*Department of Physicy, University of Illinois at Urbana-Champaign, Urbana, Illinois 61801, USA.*

We measure the thermal conductivity, heat capacity and sound velocity of thin films of five polymers, nine polymer salts and four caged molecules to advance the fundamental understanding of the lower and upper limits to heat conduction in amorphous macromolecules. The thermal conductivities vary by more than one order of magnitude, from 0.06 W m $^{-1}$ K $^{-1}$ for [6,6]-phenyl-C71-butyric acid methyl ester (PC71BM) to 0.67 W m $^{-1}$ K $^{-1}$ for poly(vinylphosphonic acid calcium salt) (PVPCa). Minimum thermal conductivity calculated from the measured sound velocity and effective atomic density is in good agreement with the thermal conductivity of macromolecules with various molecular structures and intermolecular bonding strength.

I. INTRODUCTION

Heat conduction in electrically insulating, amorphous materials can be viewed as the diffusion of vibrational energy on a time scale of 1/2 vibration period.[1, 2] The thermal transport model based on this picture, originally proposed by Einstein[3] and later extended to incorporate a Debye density of vibrational states,[1] is often referred to as the minimum

thermal conductivity model (MTCM). MTCM is in good agreement with the measured thermal conductivities of many amorphous inorganic solids[2], highly disordered crystals[1] and amorphous macromolecules. For example, MTCM accurately predicts the pressure dependence of the thermal conductivity of poly(methyl methacrylate) (PMMA),[4] and the scaling of thermal conductivity with sound velocity for several water-soluble polymers.[5] Although the disagreement between the predicted and measured values is often 20% to 40%, MTCM has the advantages of using only two easily measured variables (i.e., the atomic density and average sound velocity) to describe the complex reality of heat conduction in macromolecules.

The minimum thermal conductivity based on MTCM is

$$\Lambda_{\min} = (\frac{\pi}{6})^{1/3} k_B n^{2/3} \sum_{i=1}^{3} V_i (\frac{T}{\Theta_i}) \int_0^{\Theta_i/T} \frac{x^3 e^x}{(e^x - 1)^2} dx , \quad (1)$$

where k_B is the Boltzmann constant; n is the atomic density; $V_1=V_l$ and $V_{2,3}=V_t$ are the longitudinal and transverse speed of sounds, respectively; $\Theta_i = V_i(\hbar / k_B)(6\pi^2 n)^{1/3}$ is the Debye cut-off temperature, and $\hbar$ is the reduced Plank constant. In the high temperature limit, [4]

$$\Lambda_{\min} = (\frac{\pi}{48})^{1/3} k_B n^{2/3} (V_l + 2V_t) . \quad (2)$$

The dependence of thermal conductivity on atomic density and average sound velocity offers a practical guide for searching for the upper and lower limit of the thermal conductivity of amorphous macromolecules. Since diamond possesses the largest atomic density ($n = 1.76 \times 10^{23}$ cm^{-3}) and sound velocity ($V_l = 17500$ m s^{-1} and $V_t = 12800$ m s^{-1}) of any material,[6] we expect that thermal conductivity of pure sp3-bonded amorphous diamond (estimated as ≈ 4 W m^{-1} K^{-1}) represents the upper limit of heat conduction.[7] In

contrast, the highest value reported for an amorphous macromolecular material is about an order of magnitude smaller (≈ 0.4 W m^{-1} K^{-1} for poly(acrylic acid) and polyacrylamide).[5, 8] Regarding the lower limit, we attribute Λ_{min} of cesium iodide (CsI, 0.14 W m^{-1} K^{-1}) as the benchmark, due to the small (if not the smallest) combined values of n (2.09 x 10^{22} cm^{-3}) and *V* (V_l = 2000 m s^{-1} and V_t = 713 m s^{-1}).[9] Recently, fullerene derivatives such as [6,6]-phenyl-C61-butyric acid methyl ester (PC61BM) and [6,6]-phenyl-C61-butyric acid n-butyl ester (PCBNB) were discovered to have thermal conductivities (≈ 0.06 W m^{-1} K^{-1}) well below this benchmark.[10, 11] However, their atomic density (n = 8.8 x 10^{22} cm^{-3}) and speed of sound (V_l = 2800 m s^{-1}) are only modest. MTCM predicts a thermal conductivity of fullerene derivatives that is significantly larger than what is observed. The discrepancy is attributed to localization of vibrational states in fullerenes that decreases the number of vibrational modes participating in heat conduction. [12]

The objectives of our study are to advance the fundamental understanding of the lower and higher limit of thermal conductivity for amorphous macromolecules, and to explore the relationship between molecular structure, thermal conductivity, heat capacity and elastic constant. Heat conduction in macromoelcules is inherently complex,[13, 14] and can be affected by the atomic compositions, molecular weight, degree of branching, backbone structure and side-chain structure. We focus our exploration on the effects of intermolecular bonding and structure-induced localization of vibrational states to the thermal conductivity. We investigated five polymers and nine polymer salts with a variety of types of intermolecular bonds, and four molecules with different sizes of cages in their molecular structure. The thermal conductivities are found to vary by more than

one order of magnitude, from 0.06 W m^{-1} K^{-1} to 0.67 W m^{-1} K^{-1}. The values are in good agreement with the calculated Λ_{min} using the measured sound velocity and an effective atomic density that accounts for localization effects.

II. EXPERIMENTAL DETAILS

A. Sample preparation

We prepared thin films of polymer and polymer salt via spin-coating or spin-coating followed by ion-exchange reactions. As-received poly(acrylic acid) (PAA, powder, Mv = 450 kg mol^{-1}, Sigma-Aldrich), poly(acrylic acid sodium salt) (PANa, water solution, Mw = 15 kg mol^{-1}, Sigma-Aldrich), poly(vinylphosphonic acid) (PVPA, water solution, Mw = 24 kg mol^{-1}, Polysciences), Poly(vinylsulfonic acid sodium salt) (PVSNa, water solution, Sigma-Aldrich), poly(diallyldimethylammonium chloride) (PDDA, water solution, Mw = 200 ~ 350 kg mol^{-1}, Sigma-Aldrich), poly(allylamine hydrochloride) (PAH, powder, Mw = 450 kg mol^{-1}, Sigma-Aldrich) were dissolved or diluted by deionized (DI) water to form polyelectrolyte solutions. Poly(acrylic acid lithium salt) (PALi) and poly(vinylphosphonic acid lithium salt) (PVPLi) were obtained by titrating the PAA and PVPA solutions with lithium hydroxide (Sigma-Aldrich) to a pH of 7 or 8, respectively. Polymerization of 2-methacryloyloxyethyl phosphorylcholine (MPC, Sigma-Aldrich) yielded PMPC. Specifically, MPC (5g, 16.9 mmol, washed by diethyl ether before use) and 4,4′-azobis(4-cyanovaleric acid) (ACVA, Sigma-Aldrich, 14 mg, 0.05 mmol) were dissolved in trifluoroethanol (10 ml) followed by purging with N_2 for 30 min. The polymerization was carried out at 75 ^{o}C for 20 h. The polymer was precipitated in acetone three times and dried under vacuum, and then dissolved in DI water to make the polyelectrolyte solution.

The polyelectrolytes have concentrations ranging from 50 mg mL^{-1} to 100 mg mL^{-1}. Spin-coating of the solution on Si substrates with speeds of 2000 rpm ~ 5000 rpm yields thin films with thicknesses ranging from 100 nm to 200 nm. Prior to spin-casting, the Si substrates were cleaned sequentially by acetone (sonication for 5 min), IPA (sonication for 5 min), DI water and IPA. UV-ozone treatment[15] of the substrates for ≈10 min removed hydrocarbons adsorbed on the surfaces and made the surfaces hydrophilic. After spin-coating, the remaining water in the thin films was removed by baking the samples at 90 ^{o}C in air for 30 min.

Since ionically cross-linked polymer salts such as poly (acrylic acid calcium salt) (PACa), poly (acrylic acid iron salt) (PAFe), poly (acrylic acid copper salt) (PACu), Poly(vinylphosphonic acid magnesium salt) (PVPMg) and Poly(vinylphosphonic acid calcium salt) (PVPCa) are water-insoluble, we prepared these materials using ion-exchange of the alkali metal ions in thin films of PANa or PVPLi with the cross-linking metal ions.[16] The process started by drop-casting a methanol/water (volume ratio 7:3) solution of the corresponding metal salts (i.e. $CaCl_2$, $FeCl_3$, $CuCl_2$ or $MgCl_2$, with 1M or saturated concentration) onto the spin-casted thin-films. We allowed the solution to sit on the samples for 5 min before removing it by tilting the samples. The samples were subsequently baked at 90 ^{o}C for 2 min. We finally soaked the samples in a water bath for 2 to 3 min to remove excess salts and baked them at 90 ^{o}C for 20 min to evaporate the water.

We prepared caged molecules by spin-coating or thermal evaporation. Polystyrene (PS, Mw = 400 kg mol^{-1} and 2 kg mol^{-1}, Sigma-Aldrich), dodecaphenyl silsesquioxanes (DSQ, Mw = 1550 g mol^{-1}, Sigma-Aldrich) and [6,6]-phenyl C71 butyric

acid methyl ester (PC71BM, Mw = 1030 g mol^{-1}, Nano-C) were dissolved in toluene at a concentration of ≈ 20 mg mL^{-1} to 30 mg mL^{-1}. Spin-coating the solutions of caged molecules on pre-cleaned Si substrates followed by baking the samples at 90 ^{o}C for 30 min yielded thin films with thickness of ≈ 100 nm. We thermally evaporated (3-glycidyl) propoxy-heptaisobutyl silsesquioxanes (GHSQ, Mw = 931 g mol^{-1}, Sigma-Aldrich) and 4,4′-(1,3-adamantanediyl) diphenol (ADP, Mw = 320 g mol^{-1}, Sigma-Aldrich) onto cleaned Si substrates at a pressure of ≈ 10^{-7} Torr to form ≈ 100 nm thick thin films.

The surface roughness of the thin films was measured as < 5 nm by atomic force microscopy (AFM) on areas of 5 × 5μm^2.

B. Sample characterization

We used spectroscopic ellipsometry (J. A.Woollam VASE) to measure the thicknesses of polymers, polymer salts and caged molecules. The thickness of PC71BM was measured by X-ray reflectivity (XRR).

Hydrophilic polymers and polymer salts (such as PAA, PALi, PANa, PACa, PAFe, PACu, PVPH, PVPLi, PVPMg, PVPCa, PDDA, PAH and PMPC) tend to absorb water moistures from air and swell. To obtain the thicknesses at dry-state, we mounted a homebuilt heating stage onto the ellipsometry for the measurement at elevated temperatures. Specifically, the hydrophilic samples were first baked at 90 ^{o}C for 2 hours in a vacuum chamber (pressure of ~ 10^{-4} Torr). Then the samples were transferred to the heating stage for thickness measurement at RT and 90 ^{0}C. We found that the thicknesses measured at two temperatures has relatively large discrepancies for PDDA (24%), PAH (23%), PANa (15%), PMPC (14%), PVPH (11%); mild discrepancies for PVASNa (7%); and small discrepancies for PAA (3%), PACa(3%), PVPLi (3%), PALi (1%),

PVPCa(1%). In practice, we interpreted the values measured at 90 ^{o}C as the dry-state thicknesses.

We used quartz crystal microbalance (QCM 200, 5 MHz AT-cut quartz crystal, Stanford Research Systems) to measure the density of PALi, PANa, PACa, PVPH, PVPLi, PVPCa, PVASNa, DSQ, PC71BM and ADP. Specifically, we detected the change of resonant frequency ($\Delta\omega$) for the quartz crystal before and after spin-coating or evaporation of a designated thin film on it. The thickness of the thin film (h, typically> 200 nm) was measured by ellipsometry. The density of the film (ρ) can be calculated as $\rho = \frac{\Delta\omega}{C_f h}$, where C_f is the sensitivity factor for the crystal (56.6 Hz μg^{-1} cm^2 at room temperature). The variations in our measurements of $\Delta\omega$ are ≈ 30 Hz, which corresponds to an uncertainty of ≈ 3% for the measurement of film density.

C. Measurement of thermal conductivity and heat capacity

Time-domain thermoreflectance (TDTR), an ultrafast-laser-based pump-probe technique, enables the measurement of both thermal conductivity (Λ) and heat capacity (C) of thin films.[17, 18] A mode-locked Ti:sapphire laser produces a train of pulses (wavelength ≈ 785 nm, repetition rate ≈ 80 MHz) that is separated into a pump beam and a probe beam. An electro-optic modulator (EOM) chops the pump beam with a frequency (f) before the beam passes through a delay stage to change the optical path relative to that of the probe beam. A 5X objective lens with a $1/e^2$ radius of ≈ 10.7 μm focuses both the pump (≈ 12 mW) and probe beam (≈ 6 mW) on the sample surface. The pump beam heats the sample, and the probe beam functions as a thermometer by detecting the changes in sample reflectivity due to the temperature rise. All measurements were

performed under ambient condition, and the steady-state heating due to laser heating is calculated < 7K.

Prior to the measurement, a thin layer of Al optical transducer (≈90 nm) was deposited (via magnetron sputtering) onto the sample. The water contents in the sample after Al coating were expected as negligible, due to the long-time pumping in vacuum before deposition (90 ^{o}C baking for 2 hours at 1x10^{-4} Torr, followed by pumping at < 10^{-7} Torr overnight). The Al coating prevents the water vapor from diffusing into the sample. To check these assumptions, we used AFM to verify the thicknesses of several hydrophilic samples (PANa, PALi, PVPH, MCP, PDDA). A portion of the polymers was scratched off the substrate by a razor blade before Al deposition to create a step edge that facilitates the AFM measurement. We found that the height of the step edges matched with the thicknesses measured by ellipsometry at 90 ^{o}C to within the combined experimental uncertainties of < 8 nm.

In a TDTR measurement, we analyze the ratio of in-phase (V_{in}) and out-of-phase (V_{out}) signals of the reflected probe beam recorded by an radio frequency (RF) lock-in amplifier with the reference frequency set at *f*. Changing the modulation frequency *f* between 1 MHz to 9 MHz allows us to modify the sensitivity of V_{in}/V_{out} with respect to Λ and C for thin films with thicknesses of ≈ 100 nm to ≈ 200nm.[5, 11] We typically acquire data for V_{in}/V_{out} at three modulation frequencies, 1.1 MHz, 5.1 MHz and 9.1 MHz as a function of pump-probe delay time from -25 ps to 3600 ps.

To extract Λ and C from the TDTR data, we used a heat diffusion model to fit the three V_{in}/V_{out} curves simultaneously.[5] The model consists of three layers: the Al transducer, the thin film for investigation and the Si substrate. All the geometric

parameters and thermal properties of the Al transducer and Si substrate are measured separately or adopted from literature values; the only fitting variables are Λ and C of the thin film. The effects of the interfacial thermal conductance for the Al/polymer and polymer/Si interfaces are small since the Kapitza lengths of the interfaces are in the order of a few nm.[19] We therefore set both of the interfacial conductance to a nominal value of 100 MW m^{-2} K^{-1} in the modeling.

We validated the TDTR measurements by testing a reference sample of poly(methyl methacrylate) (PMMA). The extracted Λ and C are 0.19 ± 0.02 W m^{-1} K^{-1} and 1.60 ± 0.15 J cm^{-3} K^{-1}, respectively, which is consistent with prior studies.[5, 11, 20, 21]

D. Measurement of sound velocity

We measured the longitudinal speed of sound (V_l) for the thin films by picosecond acoustics. The echoes from Al/polymer interface (at delay time t_1) and polymer/Si interface (at delay time t_2) were detected and V_l was calculated as $(h/2)/(t_2 - t_1)$. We were not be able to find the acoustic echoes for DSQ and GHSQ, and measured V_l of DSQ and GHSQ by picosecond interferometry instead.[22]

The transverse speed of sound (V_t) was measured by the generation and detection of surface acoustic waves (SAW).[5, 23] An elastomeric optical phase-shift mask made from polydimethylsiloxane (PDMS) was first attached to the top surface of the sample. The optical mask spatially modulates the pump beam to generate SAW that were then detected by the probe beam. Based on the grating period and oscillation frequency of the signal, the velocity of the SAW (V_{SAW}) could be extracted. To obtain V_t, we used a Green's function method to model the V_{SAW} for the layered structure (Al/polymer/Si). We assume that the thin film is elastically isotropic, and all the elastic properties of the

materials are measured or known from literature values, i.e. the only unknown in fitting the calculated and measured value of V_{SAW} is V_t.

III. RESULTS AND DISCUSSION

A. Toward high thermal conductivity: effect of intermolecular bonding strength

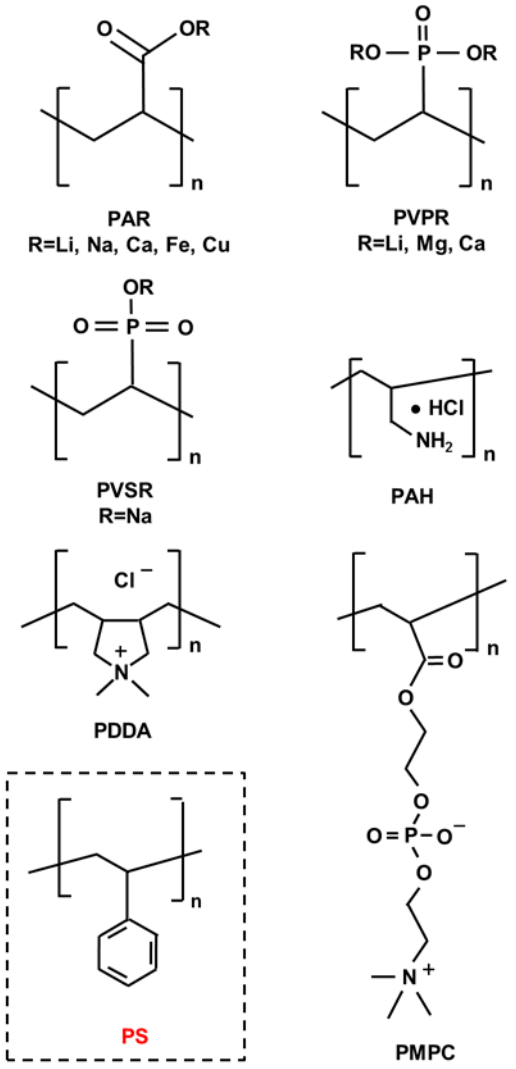

FIG. 1. Chemical structures of six types of polyelectrolytes studied for the thermal conductivity, heat capacity and sound velocity. Polystyrene is included as a reference.

Figure 1 shows the structural formula for the six types of polymers and polymer salts we investigated. Due to the presence of charged groups in the structures, these

macromolecules are often referred to as polyelectrolytes. Poly(acrylic acid R salt) (PAR, R = Li, Na, Ca, Fe, Cu), poly(vinylphosphonic acid R salt) (PVPR, R = Li, Mg, Ca) and poly(vinylsulfonic acid R salt) (PVSR = Na) are anionic polyelectrolytes with negatively charged groups in the side chain; PDDA and PAH are cationic polyelectrolytes with positively charged groups in the backbone and side chain, respectively; and PMPC is a zwitterionic polyelectrolyte because it contains both positive and negative charges in the side chains. Due to the presence of strong hydrogen bonds or ionic bonds that enhances the intermolecular thermal transport, we expect these amorphous macromolecules to have relatively high thermal conductivities.

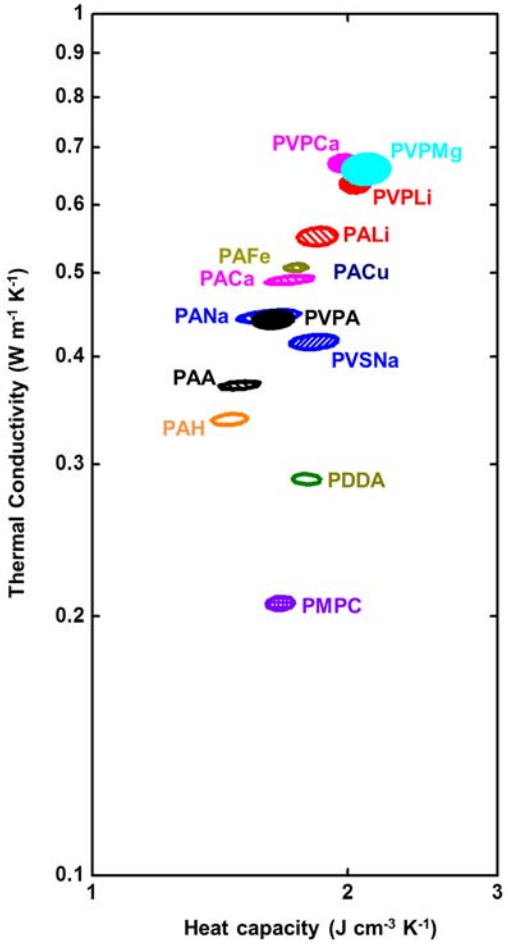

FIG. 2. Contour plot of thermal conductivity and heat capacity for the thin films of polyelectrolytes in a two dimensional parameter space. The enclosed area by the contour lines stands for the measured values of a 95% confidence interval. Data of PAA is from Ref. 5.

Figure 2 shows the thermal conductivity and volumetric heat capacity for the investigated polyelectrolytes. Data for the polyacid PAA[5] and PVPA are included for comparison. The measured values are represented by contours in the two dimensional parameter space. We define the contour as the fit to the TDTR data using the thermal model that yields a sum of normalized squared residuals (between the model and data) of $2\sigma_{min}$, where σ_{min} is the sum of the normalized least squared residuals (i.e. residuals from the best fit).[11] The size of the contour quantifies the experimental uncertainties, and the enclosure stands for experimental values of a 95% confidence interval. The typical overall uncertainties, obtained by adding the experimental uncertainties and systematic uncertainties (from the TDTR system and each layer of materials) in quadrature,[5] are ≈ 8% for thermal conductivity and ≈ 11% for heat capacity.

The measured thermal conductivities of polyelectrolytes vary by a factor of ≈ 3, ranging from 0.21 W m^{-1} K^{-1} to 0.67 W m^{-1} K^{-1}. In general, anionic polyelectrolytes (such as PVPR, PAR and PVSR) have higher thermal conductivities than cationic polyelectrolytes (PAH and PDDA) and zwitterionic polyelectrolyte (PMCP). Polymer salts are more thermally conductive than polyacids. Specifically, PMCP possesses the lowest thermal conductivity (0.21 W m^{-1} K^{-1}). PAH, PAA and PVPA have simple side chains and alkane backbones. Their thermal conductivities (0.34 W m^{-1} K^{-1}~ 0.44 W m^{-1} K^{-1}) are higher than those of typical amorphous polymers. The strong intermolecular hydrogen bonds within these polymers enhance the thermal transport between polymer chains.[5] Polymer salts such as PVPR (0.63 W m^{-1} K^{-1}~ 0.67 W m^{-1} K^{-1}), PAR (0.45 W m^{-}

^{1} K^{-1}~ 0.55 W m^{-1} K^{-1}) and PVSR (0.42 W m^{-1} K^{-1}) are among the most conductive polyelectrolytes. This qualitatively agrees with the fact that ionic inter-chain interactions are stronger than both the van der Waals interaction and hydrogen bonding. We find that PVPLi, PVPMg and PVPCa have similar thermal conductivities of 0.63 W m^{-1} K^{-1} to 0.67 W m^{-1} K^{-1}, which set the upper limit of the measured values. The high thermal conductivities are likely due to the presence of two bonding sites on each side chain.

In contrast, the measured heat capacities vary over a relatively small range, from 1.45 ± 0.15 J cm^{-3} K^{-1} to 2.1 ± 0.2 J cm^{-3} K^{-1}). Heat capacity and thermal conductivity show positive correlations, suggesting that high density of vibrational states facilitates thermal transport.

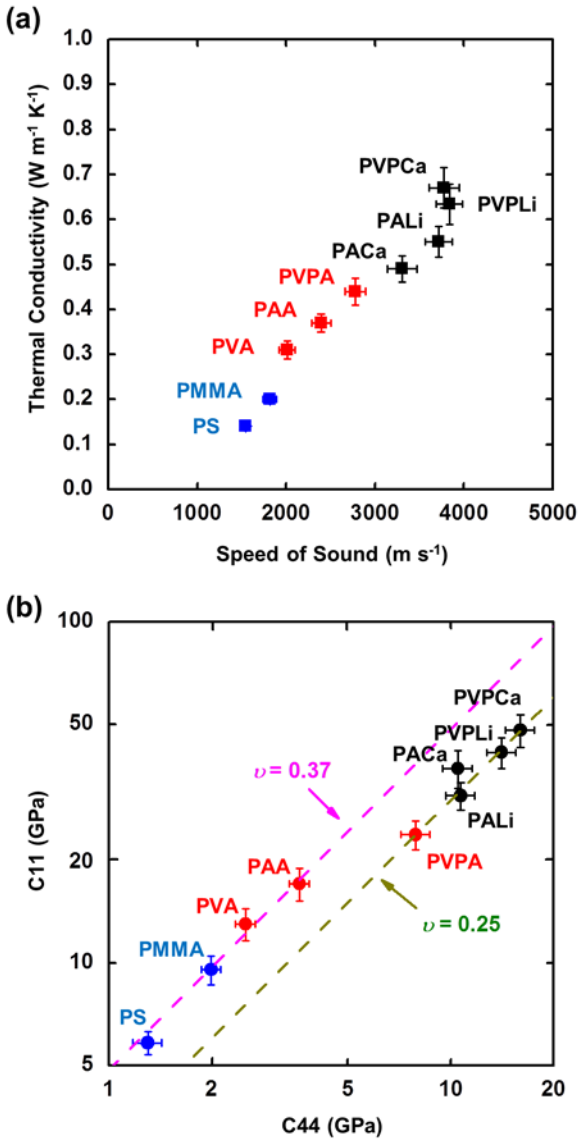

FIG. 3. (a) Measured thermal conductivity as a function of sound velocity for several polymers and polymer salts with the same backbone structures and varying inter-chain bonds: PS and PMMA (blue symbols) have van der Waals intermolecular interactions; PVA, PAA and PVPA (red symbols) possess hydrogen bonds; PALi, PACa, PVPLi and PVPCa (black symbols) are polymer salts with ionic inter-chain bonds. (b) Comparison between measured longitudinal elastic constant C_{11} and transverse elastic constant C_{44} for the macromolecules. The magenta and dark yellow dashed lines stand for a Poisson's ratio of 0.37 and 0.25, respectively. The data of PAA and PVA in (a) and (b) is from Ref. 5.

To gain insight on the effect of intermolecular bonding strength on the thermal transport, we compare the thermal conductivity, the average sound velocity (defined as $\overline{V} = \frac{1}{3}(V_l + 2V_t)$) and the heat capacity for several representative amorphous macromolecules, including PS, PMMA, PVA, PAA, PVPA, PVLi, PVCa, PVPLi and PVPCa. These macromolecules have the same alkane backbones yet different inter-chain bonds. Specifically, PS has the weakest van der Waals interactions due to the constitution of only non-polar C and H atoms. PMMA has slightly higher bonding strength because of the induced dipoles in the ester functional groups. PVA, PAA and PVPA are hydrogen bonded polymers with variations in bonding strength: bonds of PVA are weaker than that of PAA and PVPA, and the number of bonds for PVPA is larger than that of PAA and PVA. Ionic bonds in PVCa, PVLi, PVPLi and PVPCa are the strongest inter-chain interactions.

Figure 3(a) shows the thermal conductivity as well as the average sound velocity for these macromolecules. The obtained thermal conductivity varies by a factor of ≈5, and is found to correlate positively with the strength of inter-chain bonds. For example, PS has the lowest thermal conductivity (0.14 W m^{-1} K^{-1}), followed by PMMA and the three hydrogen-bonded polymers (≈0.3 W m^{-1} K^{-1} to ≈0.5 W m^{-1} K^{-1}). Thermal conductivity of the ionically bonded polymer salts is among the highest (≈0.5 W m^{-1} K^{-1} to ≈0.7 W m^{-1} K^{-1}). If we compare the thermal conductivity of PVPCa to that of PMMA under pressure,[4] the effect of ionic bonds is equivalent to adding a pressure of ≈20 GPa to the polymer with van der Waals inter-chain interactions.

Figure 3(a) also reveals the nearly linear relationship between thermal conductivity and sound velocity. This observation is consistent with Eq. (2), which

predicts the linear dependence of thermal conductivity to the product of $n^{2/3}$ and $\overline{V}$. Since heat capacity equals $3nk_B$ at the high temperature limit, we gauge n by using the measured heat capacity. While the heat capacity only varies slightly for the listed macromolecules (increases by a factor of ≈1.3 from PS to PVPCa), the average speed of sound monotonically increases with the strength of intermolecular bonds (by a factor of ≈2.5 from PS to PVPCa). Thereby, strong intermolecular interaction facilitates the exchange of thermal energy by enhancing the diffusion rate of the vibrational states, rather than by increasing the density of vibrational states participating in the transport.

Figure 3(b) shows the longitudinal elastic modulus (C_{11}) as a function of transverse elastic modulus (C_{44}) for the listed polymers and polymer salts. As the strength of inter-chain interaction increases, both C_{11} and C_{44} increase, varying by nearly an order of magnitude. The improvement in stiffness is consistent with the increase of sound velocity (Fig. 3(a)), since $C_{11} = \rho V_l^2$, $C_{44} = \rho V_t^2$, and ρ is similar for all the listed macromolecules. The modulus of PS (C_{11}= 5.8 GPa, C_{44} = 1.3 GPa) and PVPCa (C_{11} = 48 GPa, C_{44} = 16 GPa) sets the lower and upper limits of elastic constants for all the amorphous macromolecules we investigated. The increases in the mechanical rigidity with enhanced inter-chain interactions are also revealed by the Poisson's ratio ν. While for polymers with weak and intermediate inter-chain interactions, the Poisson's ratios are about 0.37; macromolecules with strong intermolecular bonds have smaller Poisson's ratio ν ≈ 0.25. The strong intermolecular bonds improves the structural connectivity and resistance to transverse contraction upon tensile loading, leading to high values of shear modulus (G) and thereby small Poisson's ratio. [24]

The elastic constants of polymer salts with divalent metal ions (e.g., PACa, C_{11} = 37 GPa) are slightly higher than those of polymer salts with monovalent metal ions (e.g., PALi, C_{11} = 31 GPa). This is consistent with the stronger ionic intermolecular bonds formed by the divalent metal ions. On the other hand, the density of PACa (1.61 g cm^{-3}) is higher than that of PALi (1.18 g cm^{-3}), which counteracts with the differences in elastic constants and yields comparable speeds of sound and thermal conductivities for PACa (V_l = 4.8 nm ps^{-1}, Λ = 0.49 W m^{-1} K^{-1}) and PALi (V_l = 5.1 nm ps^{-1}, Λ = 0.55 W m^{-1} K^{-1}).

In general, amorphous macromolecules with high speed of sound, high modulus and low Poisson's ratio tend to be more thermally conductive.

B. Toward low thermal conductivity: effect of localization of vibrational states

Among the macromolecules we studied, PS has the lowest elastic constants. Following the previous analysis, we would expect that the thermal conductivity of PS (0.14 W m^{-1} K^{-1}) sets the lower limit. However, fullerene and fullerene derivatives were reported to be less thermally conductive than PS (Λ = 0.1 W m^{-1} K^{-1} for C60 and 0.06 W m^{-1} K^{-1} for PC61BM and PCBNB).[11] Despite the ultralow thermal conductivity, the elastic constants of C60 (C_{11} = 24 GPa) and PC61BM (C_{11} = 12 GPa) are not unusually low. The discrepancy is attributed to the localization of vibrational states in the molecules with caged structures.[12] In other words, some of the excited modes contribute to the heat capacity but do not participate significantly in the transport of heat.

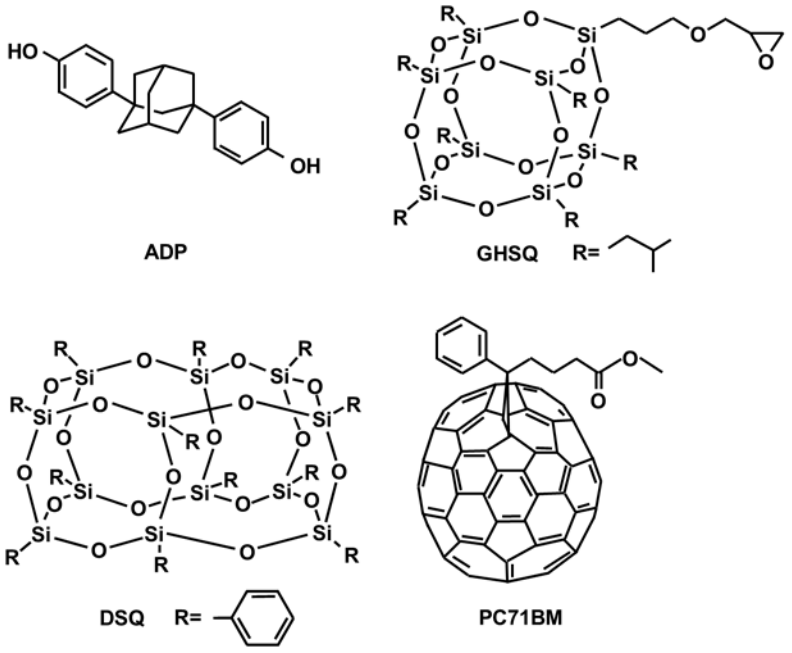

FIG. 4. Chemical structures of 4 caged molecules we studied: ADP, GHSQ, DSQ and PC71BM.

To gain further insight on the localization effects, we investigate several molecules with caged structures, including ADP, DSQ, GHSQ and PC71BM (Fig. 4). ADP is a caged organic molecule composed of one adamantane cage and two phenol groups. DSQ and GHSQ are members of silsesquioxanes which consist of an inorganic silicate cage ($[SiO_{3/2}]_n$) and organic exteriors, and are widely used in microelectronics as low-k dielectrics or lithography resists. PC71BM has a cage structure that is slightly larger than that of PC61BM, and often serves as electron acceptor materials in organic solar cells.

We do not expect a large difference in thermal conductivity between molecules and their corresponding polymers in amorphous state. The mean free path of vibrational

modes in amorphous polymers is only on the order of atomic spacing. In fact, we found that the thermal conductivity of PS-2K (molecular weight 2000, approximately 20 units of PS monomers, $\Lambda = 0.14 \pm 0.01$ W m^{-1} K^{-1}) is the same as PS-400K (molecular weight 400,000, $\Lambda = 0.15 \pm 0.01$ W m^{-1} K^{-1}) within experiment errors.

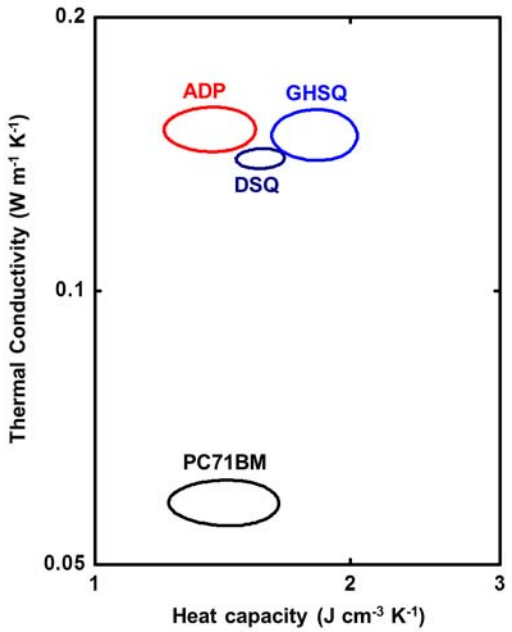

FIG. 5. Contour plot of thermal conductivity and heat capacity for the caged molecules.

Figure 5 shows the thermal conductivity and heat capacity plotted in contours of $2\sigma_{min}$ defined previously that represents 95% confidence intervals. Generally, the thermal conductivity of caged molecules is at the lower end of amorphous materials, and the values of heat capacity are within the typical range. For example, the thermal conductivity of ADP is 0.15 W m^{-1} K^{-1} and heat capacity is 1.4 J cm^{-3} K^{-1}. We found that the thermal conductivity of DSQ and GHSQ were about the same: $\Lambda = 0.14 \pm 0.01$ W m^{-1} K^{-1} for DSQ and $\Lambda = 0.15 \pm 0.01$ W m^{-1} K^{-1} for GHSQ. The thermal conductivity of PC71BM ($\Lambda = 0.06 \pm 0.006$ W m^{-1} K^{-1}) matches with that of PC61BM ($\Lambda = 0.07 \pm 0.007$ W m^{-1} K^{-1}) and PCBNB ($\Lambda = 0.06 \pm 0.007$ W m^{-1} K^{-1}).[11] The caged molecules

investigated here have similar elastic constants (e.g. C_{11} ranges from 10 GPa to 15 GPa) and Poisson' ratio (≈ 0.36). Since molecules with large cage-structures have significant amount of localized vibrational modes, they display ultralow thermal conductivity.

C. Minimum thermal conductivity model for macromolecules

TABLE I. Summary of measurement results

Sample	Λ (W m^{-1} K^{-1})	C (J cm^{-3} K^{-1})	ρ (g cm^{-3})	V_l (nm ps^{-1})	V_t (nm ps^{-1})
PALi	0.55±0.03	1.8±0.1	1.18±0.06	5.1±0.2	3.0±0.1
PANa	0.45±0.03	1.6±0.2	1.38±0.07	4.1±0.3	2.5±0.1
PACa	0.49±0.03	1.7±0.2	1.61±0.08	4.8±0.3	2.6±0.1
PAFe	0.51±0.03	1.7±0.1	---	5.0±0.2	---
PACu	0.50±0.03	1.8±0.1	---	4.8±0.3	---
PVPH	0.44±0.03	1.6±0.1	1.59±0.08	3.9±0.2	2.2±0.1
PVPLi	0.63±0.04	2.0±0.2	1.47±0.07	5.3±0.2	3.1±0.1
PVPMg	0.66±0.05	2.1±0.2	---	5.4±0.3	---
PVPCa	0.67±0.05	2.0±0.2	1.74±0.09	5.3±0.3	3.0±0.1
PVSNa	0.42±0.04	1.8±0.2	1.75±0.09	4.3±0.4	2.2±0.2
PDDA	0.29±0.03	1.8±0.2	---	3.7±0.3	---
PAH	0.34±0.03	1.5±0.2	---	4.3±0.4	---
PMPC	0.21±0.01	1.7±0.1	---	3.3±0.2	---
PS	0.141±0.009	1.3±0.1	1.03[a]	2.38±0.07	1.12±0.05
ADP	0.15±0.01	1.4±0.2	1.24±0.06	2.85±0.09	---
DSQ	0.140±0.009	1.6±0.2	1.28±0.06	2.1±0.1	0.74±0.07

GHSQ	0.15±0.01	1.9±0.2	---	---	---
PC71BM	0.06±0.006	1.4±0.2	1.62±0.08	3.0±0.2	1.36±0.06

[a] The value is from Ref. [8].

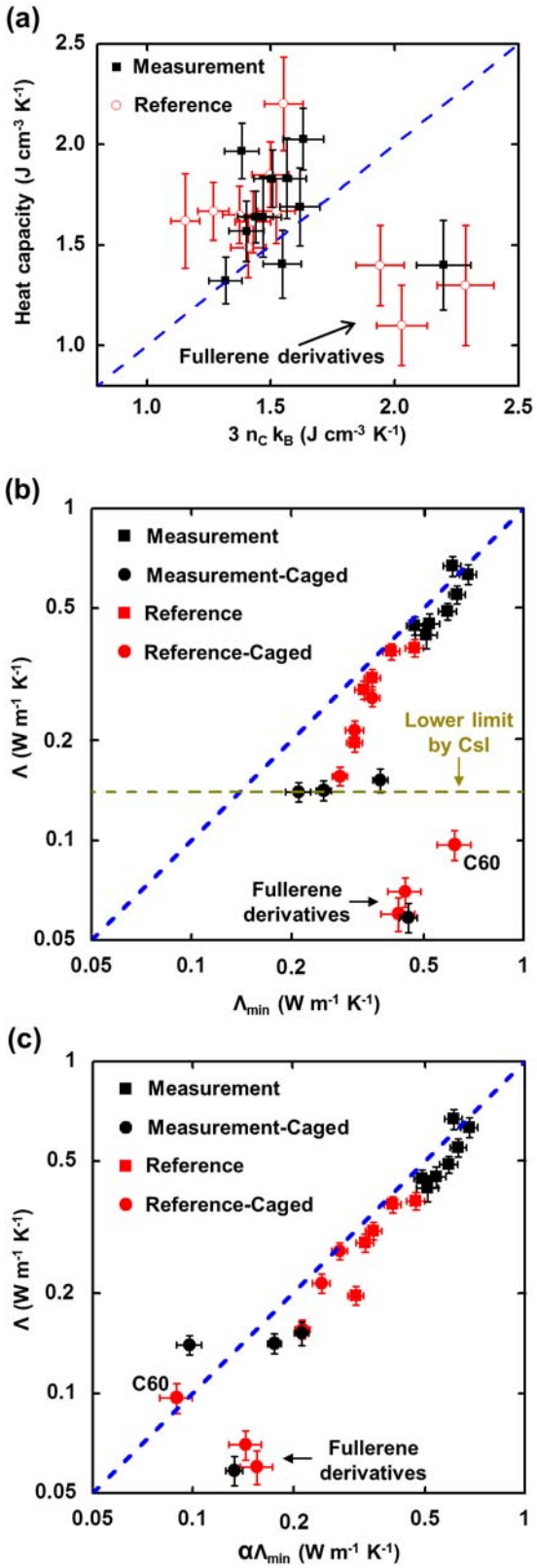
(a)
Measurement
Reference
Heat capacity (J cm-3 K-1)
3 nC kB (J cm-3 K-1)
Fullerene derivatives
(b)
Measurement
Measurement-Caged
Reference
Reference-Caged
Λ (W m-1 K-1)
Λmin (W m-1 K-1)
Lower limit by CsI
C60
Fullerene derivatives
(c)
Measurement
Measurement-Caged
Reference
Reference-Caged
Λ (W m-1 K-1)
αΛmin (W m-1 K-1)
C60
Fullerene derivatives

FIG. 6. (a) Measured heat capacity as a function of calculated heat capacity using the Debye model. Red circles are reference data including water-soluble polymers by Xie et al.[5] and fullerene derivatives by Wang et al.[11] Blue dashed line corresponds to a slope of 1. (b) Comparison of the measured thermal conductivity with the minimum thermal conductivity Λ_{min} calculated based on Eq. (1) and the estimated atomic density n_C. Red squares and red circles are data of water-soluble polymers by Xie et al.[5] and fullerene derivatives by Wang et al.,[11] respectively. Blue dashed line represents the perfect match, and dark yellow dashed line is the lower limit of minimum thermal conductivity set by CsI. (c) Measured thermal conductivity as a function of predicted minimum thermal conductivity in consideration of the localization effect. The correction factor α equals $(n_{eff} / n_C)^{2/3}$.

We summarize in Table I all the measurement results. These data enables further test of the validity of MTCM for describing heat transport in macromolecules.

One previous concern about the applicability of MTCM to macromolecules is that their vibrational spectra are quite complex, which may strongly deviate from the Debye-like spectrum of vibrational states.[4] If we calculate the nominal Debye heat capacity using the measured full atomic density ($\approx 1\times10^{29}$ m^{-3}) and sound velocity of the macromolecules, the obtained heat capacities ranges from 3 to 5 J cm^{-3} K^{-1}. The values are significantly higher than the measured ones, suggesting that the thermally excited vibrational states are overcounted. To rationally estimate the excited vibrational modes, we follow the approach of Olson et al.[25] and Wang et al.[11] For each atom (e.g. C, H, O, S, P, Si), there are three associated translational vibrational modes (total modes of 3N). Since the vibrational frequency for hydrogen-related modes and most of the bond-stretching modes are too high to excite at room temperature (RT), we exclude their contribution to heat capacity. The effective atomic density associated with heat capacity

is thereby estimated as $n_C = \frac{2}{3}(n - n_H)$, where n_H is the atomic density of hydrogen atoms.

We compare the heat capacity calculated using n_C in the Debye model to the measured heat capacity (Fig. 6(a)). For the majority of macromolecules, the calculated values are only slightly smaller (≈ 20%) than the measurements. Although details of the vibrational spectra of macromolecules are unknown, the Debye model nevertheless yields a good approximation to the sum of thermally excited vibrational modes at RT. On the other hand, estimated heat capacity of fullerene derivatives is ≈ 50 % larger than the measured values, possibly due to fact that many of the high frequency vibrational modes associated with the stiff sp2 C-C bonds are not fully thermally-excited at RT.

For evaluating the minimum thermal conductivity at RT, we use Eq. (1) and replace the full atomic density n with n_C to better quantify the number of thermally excited vibrational modes. Figure 6(b) presents the measured thermal conductivity as a function of the predicted minimum thermal conductivity. Data of water-soluble polymers from Ref. 5 and fullerene/fullerene derivatives from Ref. 10 are also included in the plot. The calculation matches well with the measurements for macromolecules with thermal conductivity in the range from ≈0.3 W m^{-1} K^{-1} to ≈0.7 W m^{-1} K^{-1} (differences within 20%). In contrast, the prediction is significantly off at the lower end, especially for the caged macromolecules. For instance, Λ_{min} of ADP is 2.4 times the measured thermal conductivity, and Λ_{min} of PC71BM is 7.7 times the measured value.

For Λ_{min} calculated using n_C and Eq. (1), all the thermally excited vibrational modes are assumed to participate in heat conduction. This treatment results in overprediction of thermal conductivity when the number of localized vibrational modes is

significant, such as the case of caged molecules. To take into account of the localization effect, we attribute each caged structure as effective 2 atoms, in consideration of the three translational and three rotational modes. The caged structures counted in this manner not only include buckyball, silsesquioxane, adamantine for the caged molecules in Fig. 4, but also contain benzene ring, lactam, pyridine and glucose that form any rigid loop structures in the caged molecules and polymers (e.g., polystyrene). This approach allows us to assess the effective atomic density n_{eff} that is directly associated with thermal transport. In general, the larger number of atoms in the rigid loop structures produces a stronger localization effect and a smaller n_{eff}. We thereby multiply Λ_{min} in Fig. 6(b) by a factor of $\alpha = (\frac{n_{eff}}{n_C})^{2/3}$ for the correction of the localization effect. For the caged molecules we investigate, α ranges from 0.30 (PC71BM) to 0.56 (ADP); and α varies from 0.68 (polystyrene) to 1 (without any rigid loop structure) for the polymers.

Figure 6(c) shows a good match (differences within ≈30%) between the measured thermal conductivity and the predictions from MTCM after the correction aforementioned. One exception is the fullerene derivatives (e.g. PC71BM), where Λ_{min} is still 2.2 times the measured thermal conductivity. The significant discrepancy between the predicted and measured values also suggests that the remaining acoustic-like modes (after eliminating the contribution of the H atom-related vibrational modes, the bond-stretching modes and the localized modes) are not fully contributing to the thermal transport. It is likely that the mismatch of vibrational density states between the buckyball and alkyl chains hinders the transport of these modes.[12]

IV. CONCLUSIONS

In conclusion, we rationally searched for the higher and lower limits of thermal conductivity among 18 amorphous macromolecules with various molecular structures and intermolecular bonding strengths. We found the highest value in ionically bonded polymer salt PVPCa (≈0.67 W m^{-1} K^{-1}), and the lowest in PC71BM with the fullerene cage structure (≈0.06 W m^{-1} K^{-1}). The measured thermal conductivity is in good agreement with the minimum thermal conductivity calculated using the measured sound velocity and effective atomic density.

ACKNOWLEDGEMENTS

This work is supported by AFOSR MURI FA9550-12-1-0002. The sample preparation and measurement were carried out in part in the Frederick Seitz Materials Research Laboratory Central Research Facilities, University of Illinois.

*To whom correspondence should be addressed. *(X.X.) E-mail: xuxie1@illinois.edu
†These authors contributed equally to this work.

1 D. G. Cahill, S. K. Watson, and R. O. Pohl, Phys. Rev. B **46**, 6131 (1992).
2 D. G. Cahill and R. O. Pohl, Solid State Commun. **70**, 927 (1989).
3 A. Einstein, Ann. Phys. **35**, 679 (1911).
4 W. P. Hsieh, M. D. Losego, P. V. Braun, S. Shenogin, P. Keblinski, and D. G. Cahill, Phys. Rev. B **83**, 174205 (2011).
5 X. Xie, D. Y. Li, T. H. Tsai, J. Liu, P. V. Braun, and D. G. Cahill, Macromolecules **49**, 972 (2016).
6 H. J. Mcskimin and W. L. Bond, Phys. Rev. **105**, 116 (1957).
7 A. J. Bullen, K. E. O'Hara, D. G. Cahill, O. Monteiro, and A. von Keudell, J. Appl. Phys. **88**, 6317 (2000).
8 J. E. Mark, *Physical properties of polymers handbook* (Springer, New York, 2006).
9 M. de Jong, et al., Sci. Data **2**, 150009 (2015).
10 J. C. Duda, P. E. Hopkins, Y. Shen, and M. C. Gupta, Phys. Rev. Lett. **110**, 015902 (2013).
11 X. J. Wang, C. D. Liman, N. D. Treat, M. L. Chabinyc, and D. G. Cahill, Phys. Rev. B **88**, 075310 (2013).
12 L. Chen, X. J. Wang, and S. Kumar, Sci. Rep. **5**, 12763 (2015).
13 D. Hands, K. Lane, and R. P. Sheldon, J. Polym. Sci. Pol. Sym. **42**, 717 (1973).

[14] T. Zhang and T. F. Luo, J. Phys. Chem. B **120**, 803 (2016).
[15] J. R. Vig, J. Vac. Sci. Technol. A **3**, 1027 (1985).
[16] M. Lahav, M. Narovlyansky, A. Winkleman, R. Perez-Castillejos, E. A. Weiss, and G. M. Whitesides, Adv. Mater. **18**, 3174 (2006).
[17] D. G. Cahill, Rev. Sci. Instrum. **75**, 5119 (2004).
[18] A. J. Schmidt, X. Y. Chen, and G. Chen, Rev. Sci. Instrum. **79**, 114902 (2008).
[19] M. D. Losego, L. Moh, K. A. Arpin, D. G. Cahill, and P. V. Braun, Appl. Phys. Lett. **97**, 011908 (2010).
[20] S. A. Putnam, D. G. Cahill, B. J. Ash, and L. S. Schadler, J. Appl. Phys. **94**, 6785 (2003).
[21] M. J. Assael, S. Botsios, K. Gialou, and I. N. Metaxa, Int. J. Thermophys. **26**, 1595 (2005).
[22] R. M. Costescu, A. J. Bullen, G. Matamis, K. E. O'Hara, and D. G. Cahill, Phys. Rev. B **65**, 094205 (2002).
[23] D. Y. Li, P. Zhao, J. C. Zhao, and D. G. Cahill, J. Appl. Phys. **114**, 143102 (2013).
[24] G. N. Greaves, A. L. Greer, R. S. Lakes, and T. Rouxel, Nat. Mater. **10**, 823 (2011).
[25] J. R. Olson, K. A. Topp, and R. O. Pohl, Science **259**, 1145 (1993).